

Rectangular Multi-Gaussian Schell-Model beams in atmospheric turbulence

This content has been downloaded from IOPscience. Please scroll down to see the full text.

2014 J. Opt. 16 045704

(<http://iopscience.iop.org/2040-8986/16/4/045704>)

View [the table of contents for this issue](#), or go to the [journal homepage](#) for more

Download details:

IP Address: 136.160.90.132

This content was downloaded on 30/04/2015 at 17:26

Please note that [terms and conditions apply](#).

Rectangular Multi-Gaussian Schell-Model beams in atmospheric turbulence

Olga Korotkova¹ and Elena Shchepakina^{2,3}

¹ Department of Physics, University of Miami, 1320 Campo Sano Drive, Coral Gables, FL 33146, USA

² Department of Technical Cybernetics, Samara State Aerospace University, Molodogvardeiskaya 151, Samara 443001, Russia

³ Department of Differential Equations and Control Theory, Samara State University, Samara 443011, Russia

E-mail: korotkova@physics.miami.edu

Received 7 January 2014, revised 6 February 2014

Accepted for publication 21 February 2014

Published 18 March 2014

Abstract

Optical beams radiated by a recently introduced class of Rectangular Multi-Gaussian Schell-Model (RMGSM) source are examined on propagation in free space and in atmospheric turbulence, with both classic and non-classic power spectra of the refractive-index fluctuations. The expression for the cross-spectral density function of such beams has been derived and used for the analysis of their spectral density (average intensity). The RMGSM beams are shown to preserve the square/rectangular shape of the transverse intensity distribution and the maximum intensity level in the flat part for relatively large distances from the source on propagation in classic turbulence. This makes the novel beams attractive for free-space optical communications and surface processing in the presence of the atmosphere.

Keywords: turbulent atmosphere, beam propagation, spectral density

PACS numbers: 42.25.Dd, 42.25.Kb

(Some figures may appear in colour only in the online journal)

1. Introduction

Among all the known classes of random beams [1–10], the recently introduced Rectangular Multi-Gaussian Schell-Model (RMGSM) beam [10] is the first one to be generated by a source with arbitrary spatial intensity distribution while forming far-field intensity distribution with rectangular symmetry. Moreover, the obtained far-field rectangular intensity pattern can have adjustable edge sharpness and is shape-invariant throughout the far zone. These properties become particularly useful in situations when a beam generated by a random source is to pass through a random medium, such as atmospheric turbulence. The deterministic beams with initial rectangular intensity profiles [11, 12] have been shown to lose their shape on propagation at some distances, even in free space, and even sooner in the presence of atmospheric turbulence. The purpose of this paper is to explore to what extent the RMGSM beams can remain shape-invariant in situations when atmospheric

turbulence is present everywhere along the propagation path of the beam.

Within the Earth's boundary layer (0–2 km above the ground) atmospheric turbulence is known to be of classic structure, i.e. to have a power law spectrum with the conventional $-11/3$ exponent [13]. Measurements of the atmospheric refractive-index fluctuations taken at higher altitudes suggest that the spatial power spectrum, while being fractal-like, can have a quite arbitrary relation with the turbulent eddy size distribution. Unlike in the boundary layer, in the various upper layers such as troposphere, tropopause and lower stratosphere, the atmospheric turbulence is shown to have a somewhat different power law and to exhibit anisotropic features [14, 15]. Turbulence with varying power law has been termed non-Kolmogorov turbulence. Hence it will also be of importance to investigate the influence of the atmospheric power spectrum's exponent on the evolution of the RMGSM beams.

2. Cross-spectral density function

Our derivation will be based on the classic coherence theory of wide-sense statistically stationary beams which are conventionally treated with the help of the mutual coherence function, or the cross-spectral density function [1]. For a RMGSM source the cross-spectral density function has the form [10]

$$W^{(0)}(\rho'_1, \rho'_2; \lambda) = \frac{1}{C^2} \exp\left(-\frac{x_1'^2 + x_2'^2 + y_1'^2 + y_2'^2}{4\sigma^2}\right) \times \sum_{m=1}^M \binom{M}{m} \frac{(-1)^{m-1}}{\sqrt{m}} \exp\left[-\frac{(x_1' - x_2')^2}{2m\delta_x^2(\lambda)}\right] \times \sum_{m=1}^M \binom{M}{m} \frac{(-1)^{m-1}}{\sqrt{m}} \exp\left[-\frac{(y_1' - y_2')^2}{2m\delta_y^2(\lambda)}\right], \quad (1)$$

where $\rho'_1 = (x'_1, y'_1)$ and $\rho'_2 = (x'_2, y'_2)$ are the 2D position vectors transverse to the direction of propagation z , λ is the wavelength of the source, $\delta_x(\lambda)$ and $\delta_y(\lambda)$ are the rms correlation widths along the x and y directions, σ is the rms source width, and $C = \sum_{m=1}^M \binom{M}{m} (-1)^{m-1} / \sqrt{m}$ is the normalization factor, where $\binom{M}{m}$ stands for the binomial coefficient.

The value of parameter M , the upper summation index of the multi-Gaussian sums (1), is responsible for the formation of the flat central part and the sharpness of the edges. For $M = 1$ the degree of coherence reduces to the classic Gaussian form, while for large M it tends to be the product of two 1D ‘sinc’ functions, $(\sin x)/x$ and $(\sin y)/y$ [10]. The correlation function in equation (1) leads to a far field with rectangular-shaped intensity distribution that is essentially a combination of the plane wave close to the beam axis and sharp Gaussian decay at the edges. Namely the resemblance of the central part of the beam to the plane wave carries the useful properties as the beam passes in random media.

According to the extended Huygens–Fresnel principle, after propagating from the source plane to points $\mathbf{r}_1 = (\rho_1, z)$ and $\mathbf{r}_2 = (\rho_2, z)$ of the half-space $z > 0$, in the presence of a linear, optically fluctuating medium, the cross-spectral density function of the beam obeys the law [13]

$$W(\rho_1, \rho_2, z; \lambda) = \frac{k^2}{(2\pi z)^2} \int_{-\infty}^{\infty} \int_{-\infty}^{\infty} W^{(0)}(\rho'_1, \rho'_2; \lambda) \times \exp\left[-ik \frac{(\rho_1 - \rho'_1)^2 - (\rho_2 - \rho'_2)^2}{2z}\right] \times (\exp[\psi^*(\rho_1, \rho'_1, z; \lambda) + \psi(\rho_2, \rho'_2, z; \lambda)])_R d\rho'_1 d\rho'_2, \quad (2)$$

where the expression in the angular brackets with subscript R is the complex phase correlation of the spherical wave in the random medium, and $k = 2\pi/\lambda$ is the wavenumber. It was shown in [16] that the phase correlation term can be well

approximated as

$$(\exp[\psi^*(\rho_1, \rho'_1, z; \lambda) + \psi(\rho_2, \rho'_2, z; \lambda)])_R \approx \exp\left\{-\frac{4\pi^4 z}{3\lambda^2} [(\rho_1 - \rho_2)^2 + (\rho_1 - \rho_2) \cdot (\rho'_1 - \rho'_2) + (\rho'_1 - \rho'_2)^2] \int_0^{\infty} \kappa^3 \Phi_n(\kappa) d\kappa\right\}, \quad (3)$$

where $\Phi_n(\kappa)$ is the 1D power spectrum of fluctuations in the refractive index of the random medium, κ being spatial frequency. Hence, the RGSM beam propagates in any linear medium according to the law

$$W(\rho_1, \rho_2, z; \lambda) = \left(\frac{k}{2\pi z}\right)^2 \times \int_{-\infty}^{\infty} \int_{-\infty}^{\infty} \int_{-\infty}^{\infty} \int_{-\infty}^{\infty} W^{(0)}(\rho'_1, \rho'_2; \lambda) dx'_1 dx'_2 dy'_1 dy'_2 \times \exp\left[-ik \frac{(x'_1 - x_1)^2 + (y'_1 - y_1)^2}{2z}\right] \times \exp\left[ik \frac{(x'_2 - x_2)^2 + (y'_2 - y_2)^2}{2z}\right] \times \exp\left\{-\frac{4\pi^4 z}{3\lambda^2} [(x_1 - x_2)^2 + (y_1 - y_2)^2 + (x_1 - x_2)(x'_1 - x'_2) + (y_1 - y_2)(y'_1 - y'_2) + (x'_1 - x'_2)^2 + (y'_1 - y'_2)^2] \int_0^{\infty} \kappa^3 \Phi_n(\kappa) d\kappa\right\}. \quad (4)$$

Using the following change of variables in equation (4):

$$x_d = x'_1 - x'_2, \quad x_s = x'_1 + x'_2, \\ y_d = y'_1 - y'_2, \quad y_s = y'_1 + y'_2,$$

we finally obtain for the propagating cross-spectral density of the RMGSM beam the formula

$$W(\rho_1, \rho_2, z; \lambda) = \left(\frac{k}{4\pi Cz}\right)^2 \times \exp\left[-\frac{ik}{2z} (x_1^2 - x_2^2 + y_1^2 - y_2^2)\right] \times W_1(x_1, x_2, z; \lambda) W_1(y_1, y_2, z; \lambda), \quad (5)$$

where

$$W_1(j_1, j_2, z; \lambda) = \exp\left[-\frac{3}{4} B(j_1 - j_2)^2\right] \int_{-\infty}^{\infty} \exp\left(-\frac{j_s^2}{8\sigma^2}\right) \times \exp\left[-\frac{ik}{2z} j_s(j_2 - j_1)\right] dj_s \times \sum_{m=1}^M \binom{M}{m} \frac{(-1)^{m-1}}{\sqrt{m}} \times \int_{-\infty}^{\infty} \exp\left[-\frac{ik}{2z} j_d(j_s - j_1 - j_2)\right] \times \exp\left[-A_{jm} j_d^2 - B\left(j_d - \frac{j_1 - j_2}{2}\right)^2\right] dj_d, \quad (6)$$

$$A_{jm} = \frac{1}{8\sigma^2} + \frac{1}{2m\delta_j^2(\lambda)}, \quad B = \frac{4\pi^4 z}{3\lambda^2} \int_0^\infty \kappa^3 \Phi_n(\kappa) d\kappa, \quad (7)$$

and $j = x, y$. The direct evaluation of the integrals in equation (6) reduces equation (5) to the form

$$\begin{aligned} W(\rho_1, \rho_2, z; \lambda) &= \left(\frac{\sigma k}{Cz}\right)^2 \exp\left[-\frac{ik}{2z}(x_1^2 - x_2^2 + y_1^2 - y_2^2)\right] \\ &\times \exp\left\{-\frac{3}{4}B[(x_1 - x_2)^2 + (y_1 - y_2)^2]\right\} \\ &\times \prod_{j=x,y} \left(\sum_{m=1}^M \frac{(-1)^{m-1}}{\sqrt{2m\left(\frac{\sigma^2 k^2}{2z^2} + A_{jm} + B\right)}} \binom{M}{m}\right) \\ &\times \exp\left[-\left(A_{jm}B(j_1 - j_2)^2 + \frac{k^2}{4z^2}(j_1 + j_2)^2\right.\right. \\ &\left.\left.+ B\frac{ik}{z}(j_2^2 - j_1^2)\right)(4(A_{jm} + B))^{-1}\right] \\ &\times \exp\left[-\left(\sigma^2 k^2 \left[2(A_{jm} + B)(j_2 - j_1)\right.\right.\right. \\ &\left.\left.\left.- \frac{ik}{2z}(j_1 + j_2)\right]^2\right)\right. \\ &\left.\times \left(8z^2(A_{jm} + B)\left(\frac{\sigma^2 k}{2z^2} + A_{jm} + B\right)\right)^{-1}\right]. \quad (8) \end{aligned}$$

In the following section we will numerically examine the evolution of the spectral density S of the RMGSM beams which can be obtained from the cross-spectral density function by the expression

$$S(\rho, z; \lambda) = W(\rho, \rho, z; \lambda). \quad (9)$$

Our discussion on propagation of the RMGSM beams in optical turbulence will be based on a fairly general model for the power spectrum characterizing atmospheric fluctuations at various altitudes [17, 18],

$$\begin{aligned} \Phi_n(\kappa) &= A(\alpha) \tilde{C}_n^2 \frac{\exp[-\kappa^2/\kappa_m^2]}{(\kappa^2 + \kappa_0^2)^{\alpha/2}}, \\ 0 \leq \kappa < \infty, \quad 3 < \alpha < 4, \quad (10) \end{aligned}$$

where the term \tilde{C}_n^2 is a generalized refractive-index structure parameter with units $m^{3-\alpha}$, $\kappa_0 = 2\pi/L_0$, $\kappa_m = c(\alpha)/l_0$, L_0 and l_0 being the outer and the inner scales of turbulence, respectively, and

$$\begin{aligned} c(\alpha) &= \left[\frac{2\pi}{3} \Gamma\left(\frac{5-\alpha}{2}\right) A(\alpha)\right]^{\frac{1}{\alpha-5}}, \\ A(\alpha) &= \frac{1}{4\pi^2} \Gamma(\alpha-1) \cos\left(\frac{\alpha\pi}{2}\right), \end{aligned}$$

with $\Gamma(\cdot)$ being the Gamma function. For the power spectrum (10) the integral in expression (7) becomes [18]

$$\begin{aligned} \int_0^\infty \kappa^3 \Phi_n(\kappa) d\kappa &= \frac{A(\alpha) \tilde{C}_n^2}{2(\alpha-2)} \left[\kappa_m^{2-\alpha} \beta \exp\left(\frac{\kappa_0^2}{\kappa_m^2}\right) \right. \\ &\left. \times \Gamma\left(2 - \frac{\alpha}{2}, \frac{\kappa_0^2}{\kappa_m^2}\right) - 2\kappa_0^{4-\alpha} \right], \quad (11) \end{aligned}$$

where $\beta = 2\kappa_0^2 - 2\kappa_m^2 + \alpha\kappa_m^2$ and $\Gamma(\cdot, \cdot)$ denotes the incomplete Gamma function. The propagation of the beam in free space can be readily obtained, as a special case, when $\tilde{C}_n^2 = 0$.

The strength of Kolmogorov and non-Kolmogorov turbulence can be assessed with the help of the generalized Rytov variance derived in [17],

$$\tilde{\sigma}_R^2(\alpha) = 1.23 \tilde{C}_n^2 k^{3-\alpha/2} z^{\alpha/2}. \quad (12)$$

We will employ this parameter to discuss the effects of the atmosphere on the RMGSM beam in the following section.

3. Numerical examples

We will now employ the derived expressions for the cross-spectral density function of the RMGSM beam to examine numerically the evolution of its spectral density in free space and in atmospheric turbulence. Unless it is specified in the figure captions the following set of parameters is used for the figures: $C_n^2 = 10^{-13} m^{3-\alpha}$, $L_0 = 1$ m, $l_0 = 1$ mm, $\sigma = 1$ cm, $\delta_{xx} = 1$ mm, $\delta_{yy} = 2$ mm, $M = 40$, $\lambda = 633$ nm. The rms source correlations δ_{xx} and δ_{yy} determine the far-field rms beam widths in the x and y directions, respectively: the larger value of the rms source correlation width corresponds to the smaller value of the far-field rms beam intensity width in the same direction.

Figures 1–3 present typical transverse cross-sections of the spectral density of the RMGSM beam propagating in free space, in Kolmogorov turbulence and in non-Kolmogorov turbulence, respectively, at six propagation distances: 10 m, 100 m, 500 m, 1 km, 5 km and 10 km from the source plane. This choice allows us to examine the beam behavior at various ranges: intermediate and far zones for free-space propagation and weak and strong atmospheric fluctuation regimes for propagation in turbulence.

In figure 1 the behavior of the spectral density S ($N^2 m^{-2}$) of the RMGSM beam in free space is shown as a function of x (m) and y (m). The rectangular profile of the beam starts to appear already at distances of the order of tens of meters (figures 1(A) and (B)). It then gradually converts to the flat-top rectangular profile (figures 1(C)–(F)). The beam preserves the rectangular shape for any range while expanding in width and decreasing in maximum value.

Figure 2 presents the behavior of the same beam as in figure 1 on propagation in Kolmogorov turbulence ($\alpha = 3.67$) with relatively strong local refractive-index fluctuations ($C_n^2 = 10^{-13} m^{-2/3}$). While the beam forms similarly to the free-space case for short distances (figures 2(A) and (B)), it is seen that on propagation further the flat center of the profile cannot be fully formed (figures 2(C) and (D)), even though the rectangle-like shape of the profile can still be seen (figure 2(C)). For distances of the order of several kilometers, the rectangular shape gradually converts to elliptical (figures 2(E) and (F)).

In figure 3 we show the evolution of the same beam in the presence of non-Kolmogorov turbulent fluctuations with $\alpha = 3.2$ ($\tilde{C}_n^2 = 10^{-13} m^{3-\alpha}$), which is about the minimum measured value [15]. Unlike in the Kolmogorov case the effect

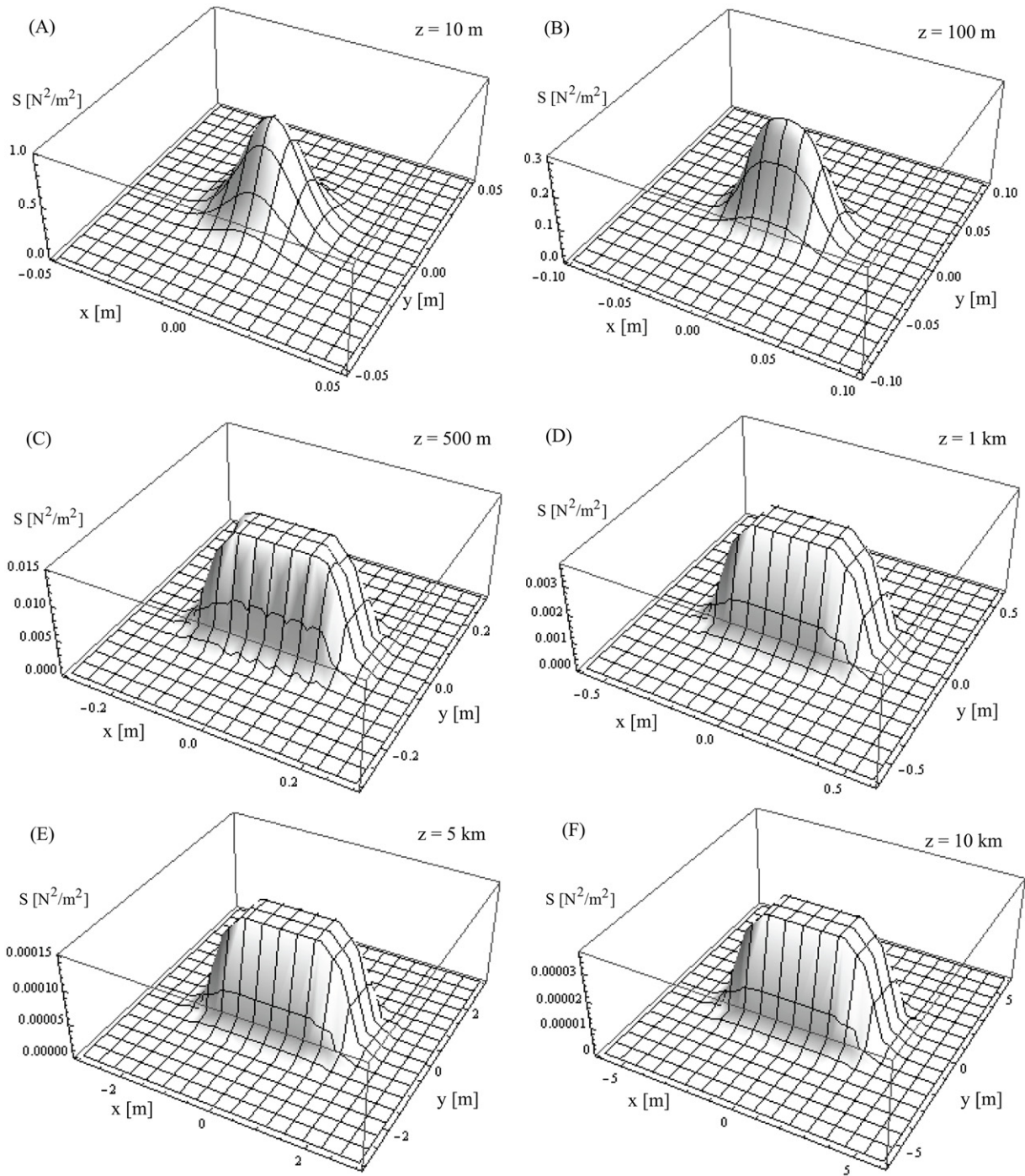


Figure 1. The spectral density of a typical RMGSM beam propagating in free space.

of turbulence here is much stronger and starts affecting the beam at shorter distances from the source. The flat profiles cannot be seen and the rectangular shape cannot be recognized at any propagation distance. The only distinctive feature of the beam—the anisotropy of the spectral density along the x and y directions—can be visually assessed, but only for sufficiently short distances from the source. As the beam enters the range of tens of kilometers (figure 3(F)) it completely loses the elliptical profile.

In figure 4 the dependence of the spectral density of the RMGSM beam on the value of the summation index M is explored in detail. For fixed propagation distance $z = 1$ km the x and y cross-sections (solid and dashed curves, respectively) of the same beam as in figures 1–3 are presented, but with (A) $M = 40$, (B) $M = 10$, (C) $M = 4$ and (D) $M = 1$ (corresponding to the classic Gaussian Schell-Model beam [1]). One can see at once that for large values of M the beam is less susceptible to the atmospheric turbulence effects. Furthermore,

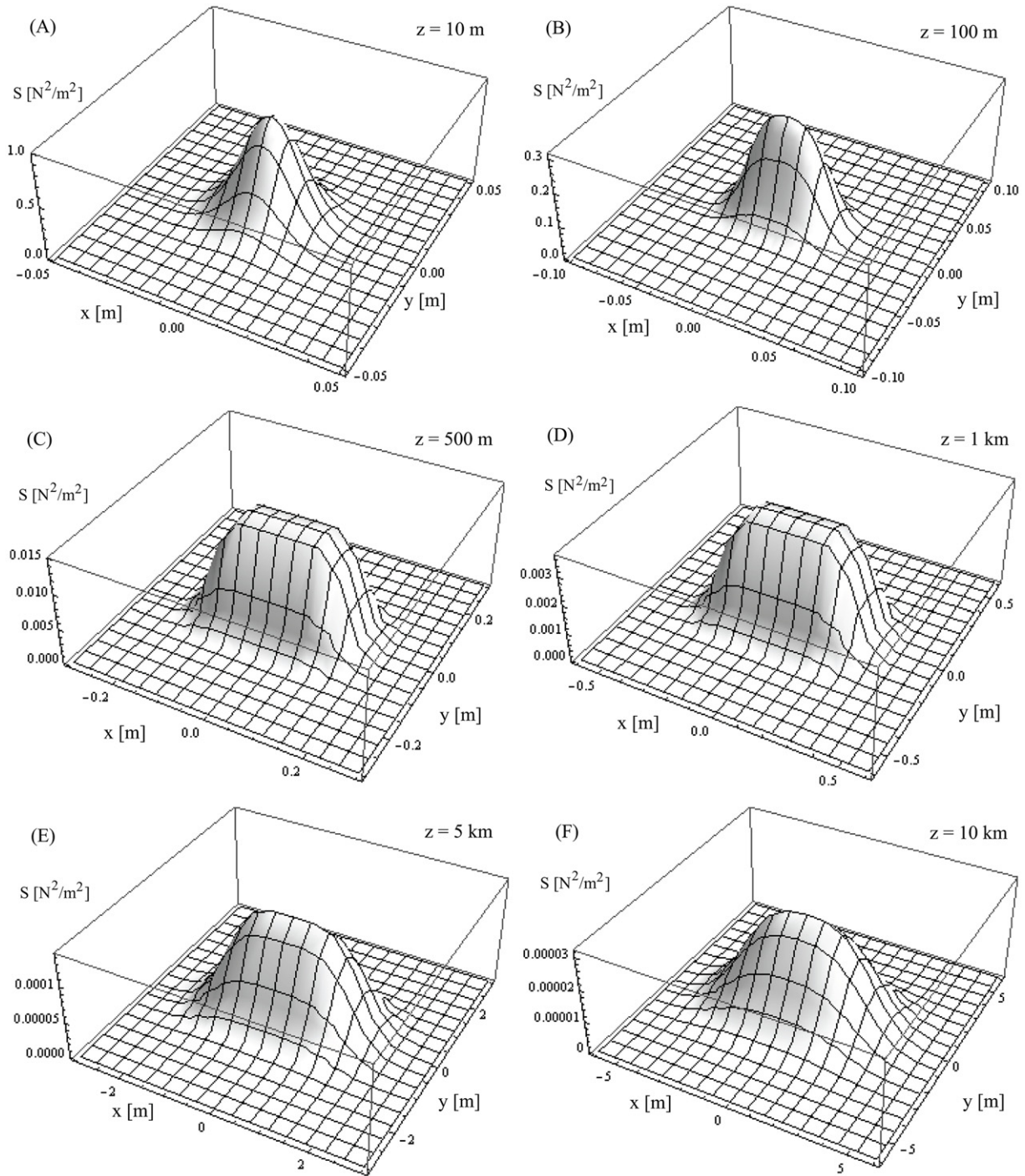


Figure 2. The spectral density of a typical RMGSM beam propagating in Kolmogorov turbulence. The Rytov variance is (A) 0.001, (B) 0.083, (C) 1.588, (D) 5.660, (E) 108.2, (F) 385.6.

in figures 4(A) and (B) the free-space curves have the same maximum value as the curves relating to the case $\alpha = 3.67$, while for $\alpha = 3.20$ the drop in the maximum intensity becomes substantial. This is not the case for lower values of M : in figures 4(C) and (D) such maximum values are lower for $\alpha = 3.67$ than for free-space propagation. One can also conclude that the non-Kolmogorov turbulence ($\alpha = 3.20$) completely destroys the hard edges of the RMGSM beam with any M .

4. Summary

The expression for the cross-spectral density function of beams generated by a novel class of RMGSM sources and propagating in free space and in atmospheric turbulence has been derived. The beams of this class are shown to gradually acquire a rectangular intensity profile towards the far zone in free space, from absolutely arbitrary initial intensity profile,

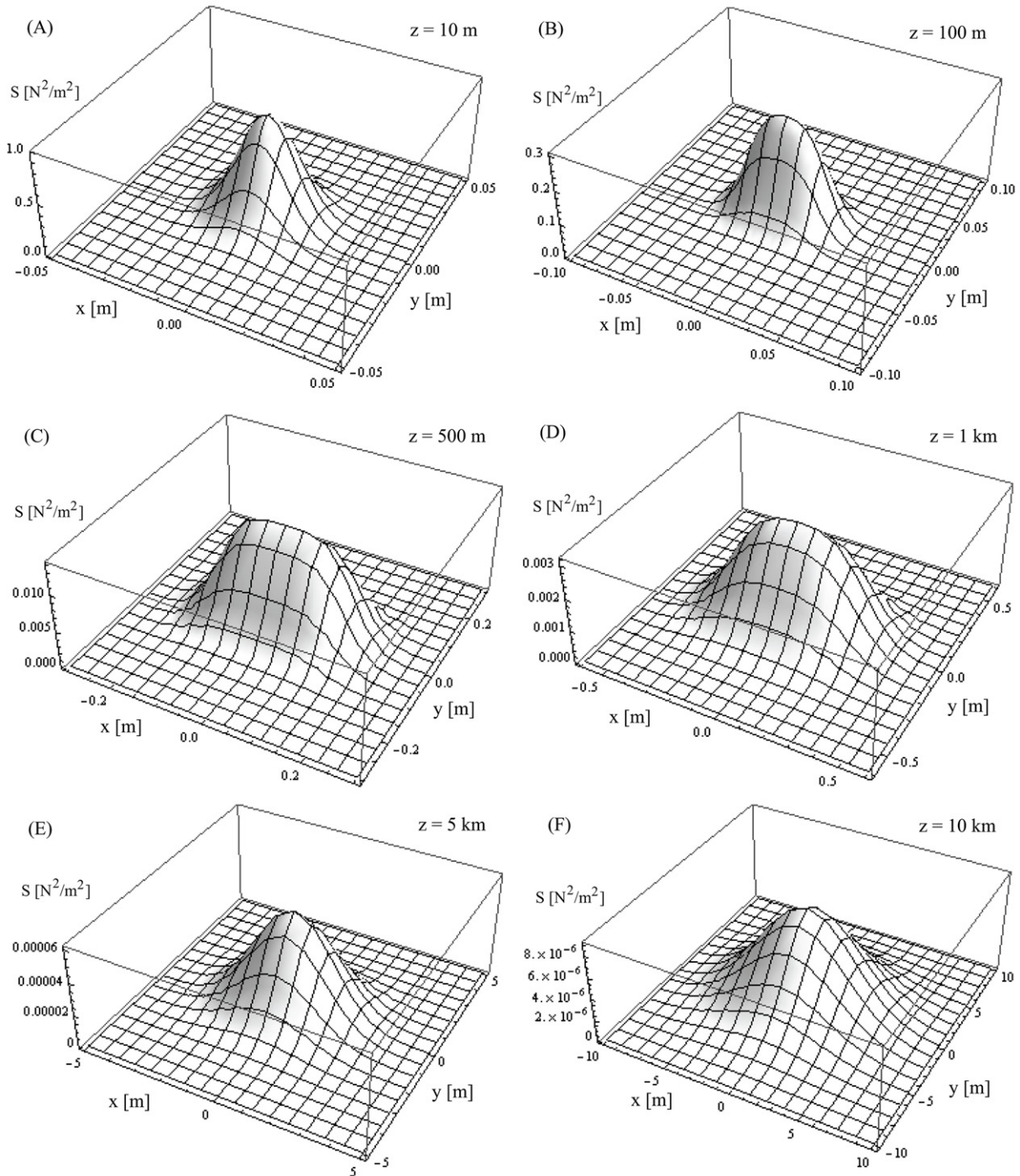


Figure 3. The spectral density of a typical RMGSM beam propagating in non-Kolmogorov turbulence. The Rytov variance is (A) 0.031, (B) 1.217, (C) 15.99, (D) 48.46, (E) 636.4, (F) 1929.

for instance Gaussian, as in our calculations. The far-field rectangular profile remains invariant in shape but scales up due to diffraction.

On propagation through the homogeneous and isotropic Kolmogorov atmosphere the RMGSM beam is shown to possess a remarkable shape robustness in the weak turbulent regime but to gradually lose the sharp corners and edges and to take on an elliptical shape on passage through strong turbulence. The beam robustness is largely determined by the

value of the upper index M in the multi-Gaussian source degree of coherence: the greater the value of M , for longer distances the shape is preserved and the intensity of the central part does not decrease. Such an effect can be explained by the fact that the flat part of the beam behaves as a plane wave which must remain constant on passage through any medium without absorption or gain. However, the effect of diffraction on the beam edges leads to gradual distortion of the flat part. It is also found that the novel beam is less resistant

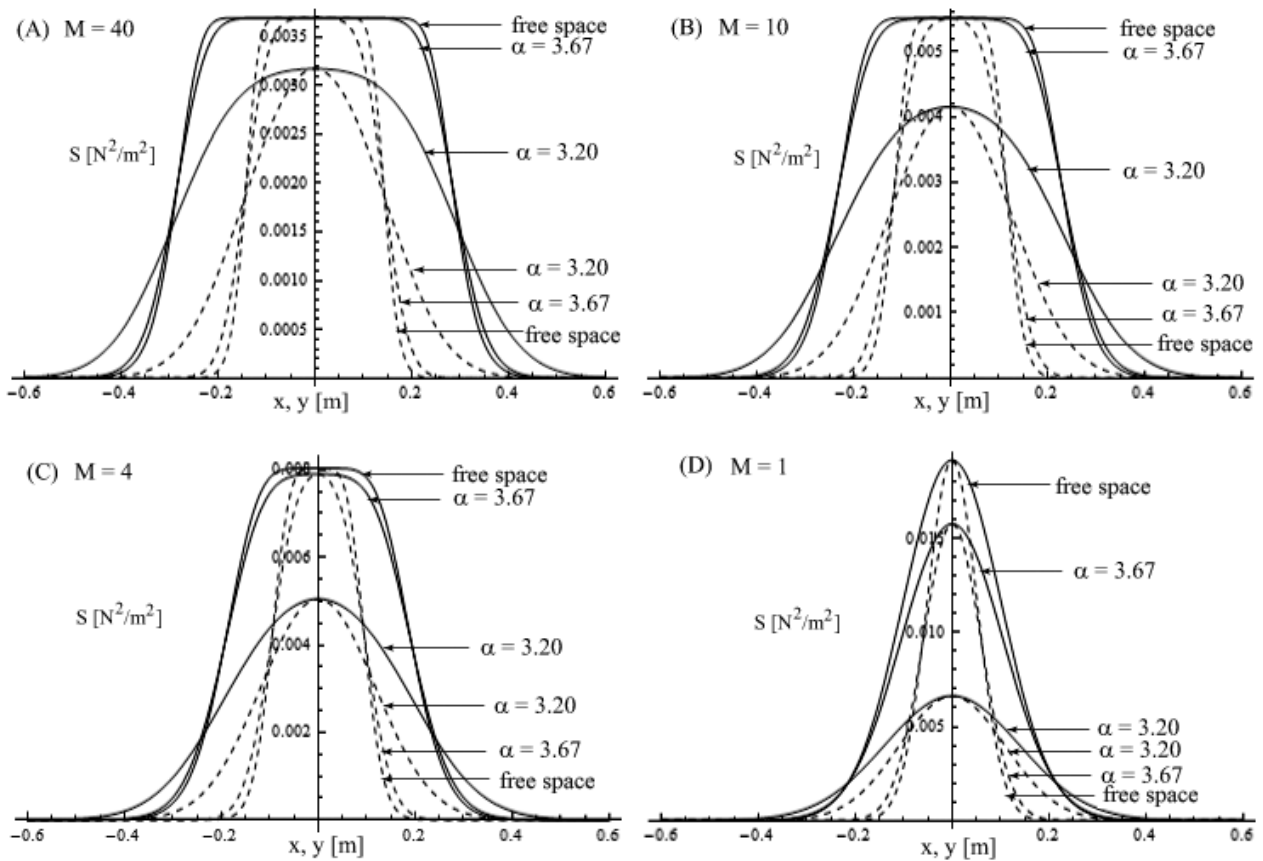


Figure 4. The spectral density of RMGSM beams with different values of M propagating in free space, Kolmogorov and non-Kolmogorov turbulence. Solid and dashed curves represent the spectral density in x and y directions, respectively.

to the effects of non-Kolmogorov turbulence. Indeed, for this type of atmosphere the sharply rectangular profile cannot be achieved at any propagation distance and the beam's intensity becomes Gaussian-like at several kilometers from the source plane, losing even its anisotropic feature.

The RMGSM beam can serve as a tool for efficient data transfer, remote sensing and material surface processing in cases when the required profile must be formed over a space from the source filled with a random medium. Our analysis can readily be adapted to other linear random media, such as oceanic turbulence and bio-tissues.

Acknowledgments

O Korotkova's research is supported by US AFOSR (FA9550-12-1-0449) and US ONR (N0018913P1226); E Shchepakina is supported in part by the Russian Foundation for Basic Research (grants 13-01-97002 p, 14-01-97018 p).

References

- [1] Mandel L and Wolf E 1995 *Optical Coherence and Quantum Optics* (Cambridge: Cambridge University Press)
- [2] Palma C, Borghi R and Cincotti G 1996 Beams originated by J0-correlated Schell-model planar sources *Opt. Commun.* **125** 113–21
- [3] Ponomarenko S A 2001 A class of partially coherent beams carrying optical vortices *J. Opt. Soc. Am. A* **18** 150–6
- [4] Lajunen H and Saastamoinen T 2011 Propagation characteristics of partially coherent beams with spatially varying correlations *Opt. Lett.* **36** 4104–6
- [5] Sahin S and Korotkova O 2012 Light sources generating far fields with tunable flat profiles *Opt. Lett.* **37** 2970–2
- [6] Korotkova O, Sahin S and Shchepakina E 2012 Multi-Gaussian Schell-model beams *J. Opt. Soc. Am. A* **29** 2159–64
- [7] Mei Z and Korotkova O 2013 Random sources generating ring-shaped beams *Opt. Lett.* **38** 91–3
- [8] Mei Z and Korotkova O 2013 Cosine-Gaussian Schell-model sources *Opt. Lett.* **38** 2578–80
- [9] Alieva T, Rodrigo J A, Cámara A and Abramochkin E 2013 Partially coherent stable and spiral beams *J. Opt. Soc. Am. A* **30** 2237–43
- [10] Korotkova O 2014 Random sources for rectangularly-shaped far fields *Opt. Lett.* **39** 64–7
- [11] Gori F 1994 Flattened Gaussian beams *Opt. Commun.* **107** 335–41
- [12] Li Y 2002 New expressions for flat-topped beams *Opt. Commun.* **206** 225–34
- [13] Andrews L C and Phillips R L 2005 *Laser Beam Propagation through Random Media* 2nd edn (Bellingham, WA: SPIE Press)
- [14] Belenkii M S, Barchers J D, Karis S J, Osmon C L, Brown J M and Fugate R Q 1999 Preliminary experimental evidence of anisotropy of turbulence and the effect of

- non-Kolmogorov turbulence on wavefront tilt statistics
Proc. SPIE **3762** 396–406
- [15] Zilberman A, Golbraikh E, Kopeika N S, Virtser A, Kupersmidt I and Shtemler Y 2008 Lidar study of aerosol turbulence characteristics in the troposphere: Kolmogorov and non-Kolmogorov turbulence *Atmos. Res.* **88** 66–77
- [16] Lu W, Liu L, Sun J, Yang Q and Zhu Y 2007 Change in degree of coherence of partially coherent electromagnetic beams propagating through atmospheric turbulence *Opt. Commun.* **271** 1–8
- [17] Toselli I, Andrews L C, Phillips R L and Ferrero V 2008 Free-space optical system performance for laser beam propagation through non-Kolmogorov turbulence *Opt. Eng.* **47** 026003
- [18] Wu G, Guo H, Yu S and Luo B 2010 Spreading and direction of Gaussian–Schell model beam through a non-Kolmogorov turbulence *Opt. Lett.* **35** 715–8